MECHANIKA
TEORETYCZNA
I STOSOWANA
3-4, 23 (1985)

THE APPLICATION OF DYNAMIC HOLOGRAPHIC INTERFEROMETRY AND PHOTOELASTICITY TO PROBLEMS IN GEOTECHNICAL ENGINEERING

D. C. HOLLOWAY, W. H. WILSON, W. L. FOURNEY, D. B. BARKER

Department of Mechanical Engineering
University of Maryland
College Park, Maryland 20742 USA.

Abstract

The methods of dynamic holographic interferometry, using a pulsed ruby laser, and dynamic photoelasticity, using a Cranz-Schardin camera, have been applied to the study of explosives and their effects in geologic applications. Specifically, the problem of stress wave generation from a surface detonation and how these stress waves interact with surface trenches was studied via holographic interferometry. This method was also applied to the examination of the shock front emitted from a non-electric detonating cord. Dynamic photoelasticity was employed to examine the role of remote discontinuities in explosive fragmentation, and in the determination of the optimum placement of explosives for gas and oil well stimulation.

Introduction

Dynamic holography and photoelasticity can be valuable tools in the study of how explosives can be more efficiently used in the civilian applications of mining, construction, and natural resource stimulation. With the emphasis today on saving costs, improving fragmentation results, improving the quality of the standing geologic material, and reducing immediate and long-term environmental effects there is a need to examine how explosives work to fracture rock. Holography and photoelasticity are convenient full field laboratory methods that provide information on the relative importance of the many blasting parameters. The results from these tests have been both quantitative and qualitative, and in many cases have been successfully scaled up for field application. This paper will focus on some recent problems that our laboratory has studied.

1. A Holographic Study of Dynamic Surface Response to Explosive Loading

Within the last several years there has been an increased need to control and reduce ground vibrations from surface blasting. As population centers have spread, the number of cases in which blasting must be done close to or even within developed areas has increased. Early studies attempted to identify characteristics of the stress waves which could be correlated to structural damage, and then to quantify safe levels of blasting based on these correlations. Another approach is to attempt to isolate structures or entire surroundings from the detonation area. Since most of the stress wave energy produced from a detonation is carried near the surface by Rayleigh type or *R* waves, it has been suggested that effective isolation can be obtained by surrounding a blast area with trenches of some depth. For a more detailed discussion of the background of this problem, see Holloway and Wilson (1983). In order to study this approach, and to quantify such parameters as trench depth, location, and effectiveness, we have made extensive use of holographic interferometry.

A complete description of the techniques used to produce photographs of dynamic surface response by holographic interferometry can be found in Holloway and Patacca (1975), and Holloway, Fourney and Patacca (1977). A pulsed ruby laser, operating at 6943 Å, was used to generate double exposure holograms of the model surface. Typical Q-switched pulse duration was 30 nanoseconds, with a 200 microsecond delay between pulses. An explosive charge of from 70 to 250 mg of PETN was detonated on the model surface at a controlled time between the two laser pulses. Specimens tested were granite blocks or cast blocks of Hydrostone, a product of United States Gypsum which when cured has a specific gravity of 1.69 and a compressive strength of 9,750 psi (67.2 mPa).

In each test, the charge was located 80 mm from a trench of rectangular cross section cut into the model surface. Trench depths of 10 mm and 18 mm were used. The illumination

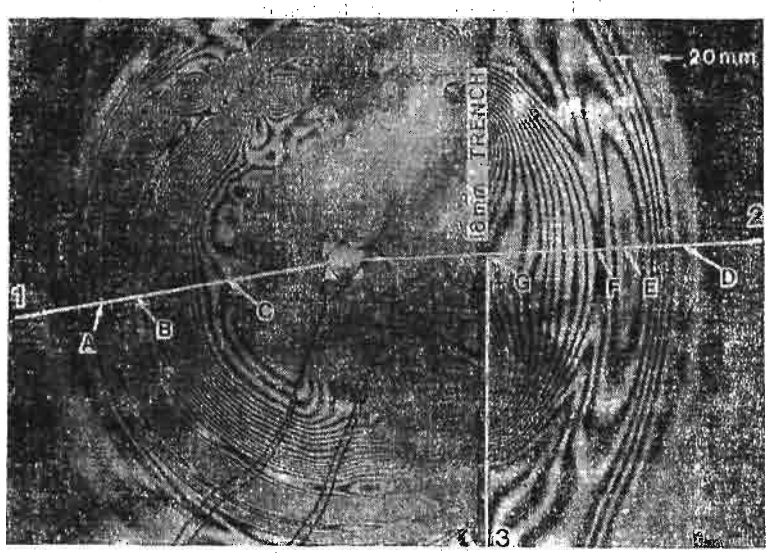

Fig. 1. *R* and *RP* wave patterns on a Hydrostone model, 90 μs after detonation. Lines *1*, *2* and *3* used in plots in Fig. 2. Points *A* through *G* (except *C*) show maximums, minimums and inflection points of the vertical surface displacement

and viewing angles were arranged so that the fringe pattern in the hologram represents a topological map of displacement normal to the model surface at the instant of the second laser pulse. Thus, we were able to study the overall effect on vertical ground motion in the waves crossing the trench. Figure 1 shows the fringe pattern 90 μs after detonation, for the case of an 18 mm trench depth. The radial lines marked 1 and 2 and a line marked 3 along the trench have been used in the analysis of the surface displacements presented in Figure 2. At the far left along line 1 (no trench) are seen remnants of a shear wave recognized by its typically asymmetric pattern. Nearer the source, the peak positive displacement of the R wave is located at point A. The region of steepest displacement gradient then follows, as can be seen from the very tight clustering of the fringes. This is also the region of highest particle velocity. A minimum or valley is reached at point B. The surface then moves upward again. The air shock front is reached at point C, and all surface interferometric information is lost inside this radius.

Moving inward along line 2 from the right, we first notice a disturbance which has no counterpart on line 1. A small positive peak is reached at point D, followed by a local minimum at E. This displacement profile is very similar to that of an R-wave. This wave shows up consistently from test to test. Analysis of the tests show its velocity to be the same as that of an R-wave, and it is found to have been located at the trench just as the P-wave passed the trench. This R type wave (precursor to the main R-wave which follows), is created by the P-wave, and will be called an RP-wave. Further in along line 2, the relative peak of the transmitted R-wave is found at point F, and its minimum at G. As can be seen from Figure 2 there is a reduction of amplitude and an increase in wavelength for the transmitted wave; this has been found to be a general result.

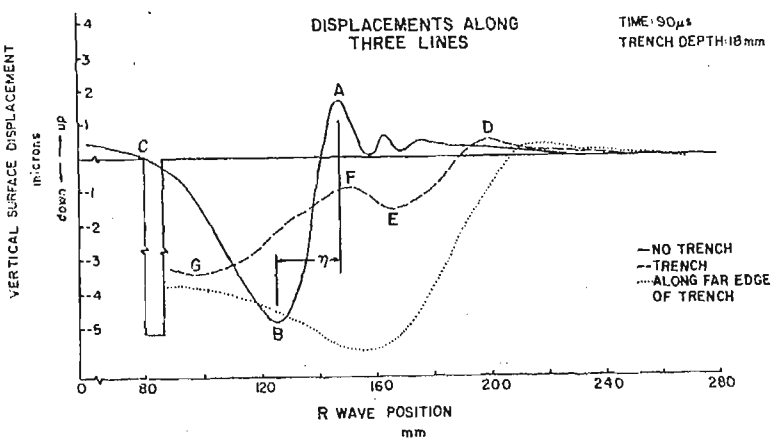

Fig. 2. Wave shapes 90 μs after detonation, along lines *1*, *2* and *3* of test shown in Figure 1. Wave position is relative to load location. Distance η is a repeatable feature in the R wave

Along line 3 on the far edge of the trench, there is at the lower end a very weak upward motion in the head of the wave followed by a downward displacement which is greater than the deepest part of the R-wave on line 1. We believe that there is another R-type wave traveling on the vertical side of the trench that is contributing to the R-wave displace-

ments on the horizontal surface. This observation points to the inadvisability of locating a structure within an R wavelength of an isolation trench.

An easily identifiable feature of the R-wave is the portion of the wavelength between the maximum upward and the deepest positions. The highest particle velocities occur in this part of the R-wave. This distance has been labeled as η in Figure 2 and is used in normalizing the results with trench depth, so that the effect of the trench can be measured. Peak particle velocities were calculated for fourteen tests, comparing R-waves on each side of the trench. The quantity (Vp-trench)/(Vp-no-trench), where Vp is peak particle velocity, is plotted in Figure 3 as a function of the ratio of trench depth H over fractional, wavelength η (H/η). The linear fit to the data in the region of analysis is good, with a least squares correlation coefficient of .995.

Figure 3 shows that trench effectiveness in R wave attenuation increases with the ratio, trench depth over wave length. Thus, for a given trench depth, the higher frequency com-

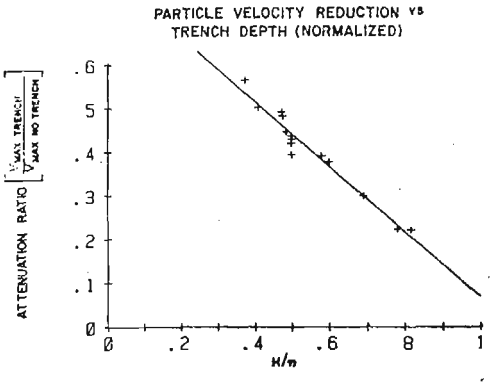

Fig. 3. Least squares linear fit for 14 tests, showing ratio of peak particle vertical velocity vs. H/η. H is depth of trench, and η is portion of wave from maximum to minimum. Typical η length is shown in Figure 2

ponents of the R-wave are more effectively attenuated. The effect of the trench on the R-wave is to reduce the overall displacement and to broaden the wave, thus lowering its frequency and reducing its particle velocity.

Our study also has identified other effects of the trench on the full wave system which should be considered in design of screening trenches. The distance of the trench from the source and trench depth are important factors, with some trade-offs involved. The P-wave, upon crossing the trench, has part of its energy converted to a new RP-wave, attenuating as $1/r^2$, while the RP-wave generated will attenuate only as $1/\sqrt{r}$. Although increasing trench depth improves R-wave blocking, it also increases the amount of P-wave energy the trench will intercept and convert to RP-wave energy. Finally, it also was observed that a high amplitude R-type wave propagates on the vertical surface of the trench.

2. Holographic Interferometry Applied to the Study of an Explosive Shock Front

Holographic methods are being used in our laboratory to study the behavior of shock fronts from various explosive detonators and initiator systems. Important parameters to be studied are the speed of the shock front, the pressure distribution behind the shock, and

the shape of the shock as it advances. The advantage of holographic techniques is that we gain information which can be related to all of these topics. Figure 4 shows a spherical shock front generated 95 μsec earlier at the end of an Ensign-Bickford Nonel detonating tube. Nonel tube is a 3 mm diameter plastic tube coated internally with a thin film of high explosive. It is used to initiate detonations from remote locations by propagating an explosive shock along the inside of the tube. It is manufactured by Ensign-Bickford using

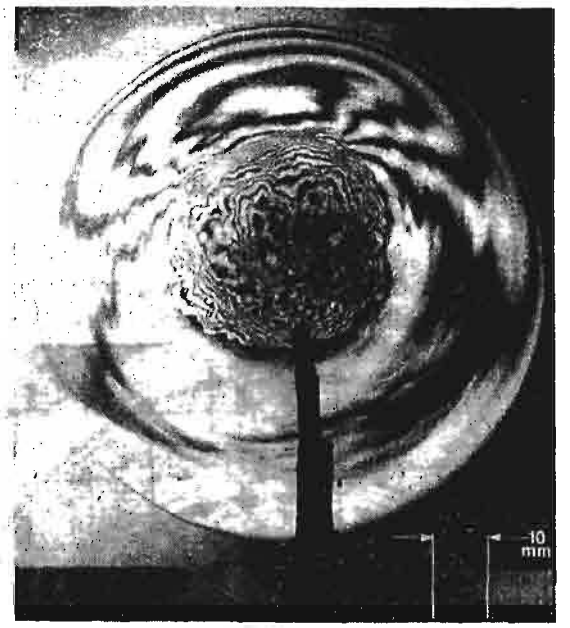

Fig. 4. Gas shock 95 s after being formed at end of Nonel detonator tube

proprietary and patented processes, under license from the Nitro Nobel Co. of Sweden, its inventor. As the explosively driven shock front propagates away from the end of the tube, the gas behind it is compressed, altering its index of refraction. Thus, the optical path is changed due to both a pressure rise and a change in the explosive gas composition. The combined effect produces interferometric fringes in the holographic image. By integration through the thickness of the spherical shock volume, we will be able to produce a pressure map of the shock intensity. Holographic interferometry can be used in a similar way to measure the strength and shape of other detonation system components, such as blasting caps and detonating cord, and to illustrate the high speed effects of these detonators on nearby components such as coupling blocks or other explosives.

3. A Dynamic Photoelastic Investigation of Fracture Initiation from Flaws Driven by Explosively Generated Stress Waves

In order to gain a basic understanding of the various fragmentation mechanisms in rock blasting, an experimental program was conducted with two dimensional polymeric models. Dynamic photoelasticity permitted the crack propagation behavior to be studied

in detail. The use of the Cranz-Schardin camera to record dynamic photoelastic fringe patterns, stress wave propagation, and crack propagation has been previously described; see for example Riley and Dally (1969). The particular example presented in this paper describes work conducted to study the initiation of cracks from flaws outside of the immediate borehole vicinity, and the contribution of these remote cracks to the overall fragmentation pattern. For a more detailed description, see Barker and Fourney (1978).

The fragmentation model was 305 mm in diameter and 6 mm thick, made from a sheet of a brittle birefringent polymer known as Homalite 100. Approximately 250 mg of PETN was tightly packed into a 6 mm diameter borehole in the center of the model. Pressure containment within the borehole was obtained with steel end caps and a lever arm arrangement that did not significantly obscure the visibility of the experiment. The explosive was detonated while the model was in a light field polariscope, and a Cranz-Schardin multiple spark gap camera recorded the dynamic photoelastic fringe patterns.

Figure 5 is a photo of the model 65 μsec after the explosive was detonated. The fringes of the outgoing *P*-wave are just about to reach the model boundary. The dark vertical shadows extending upward from the center of the model are the arms which hold the pressure containment caps over the borehole. At each grid intersection in the model small

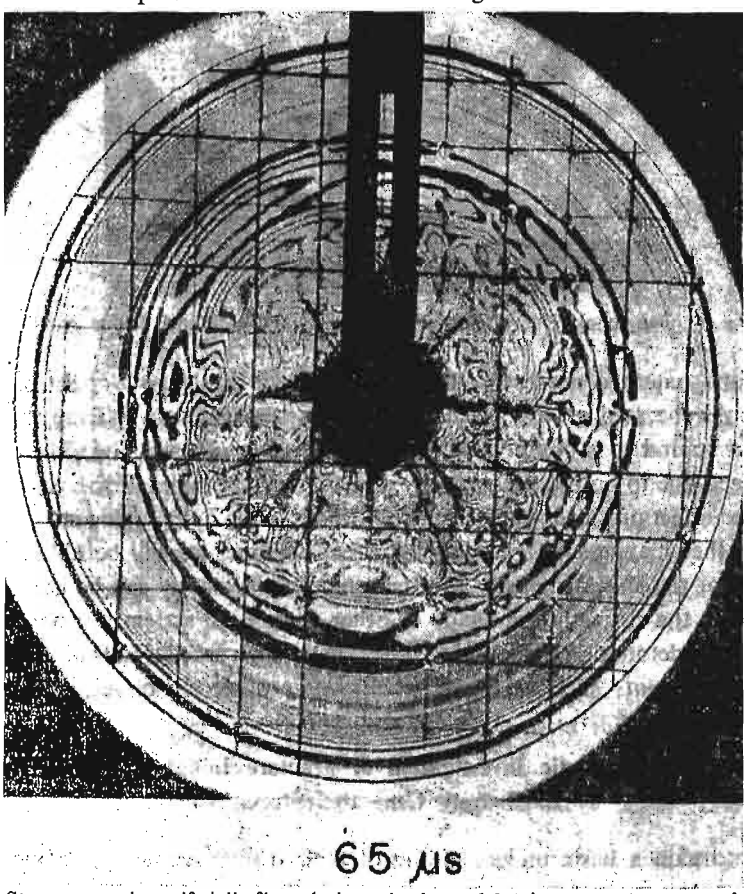

Fig. 5. and 6. Stress waves in artificially flawed photoelastic model. Time after detonation is shown. Note crack formation and growth at each flaw

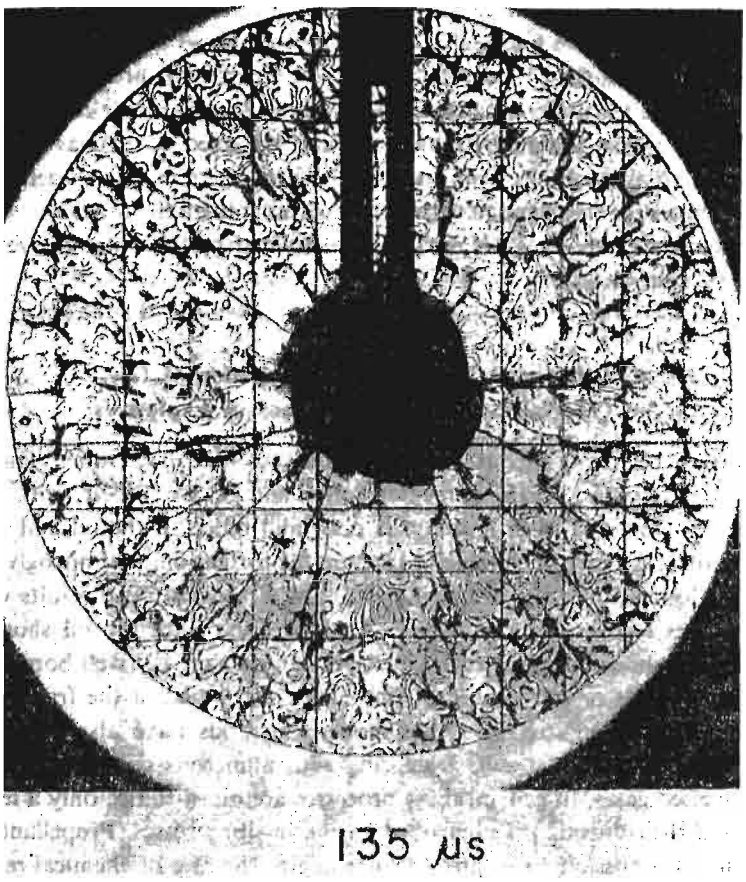

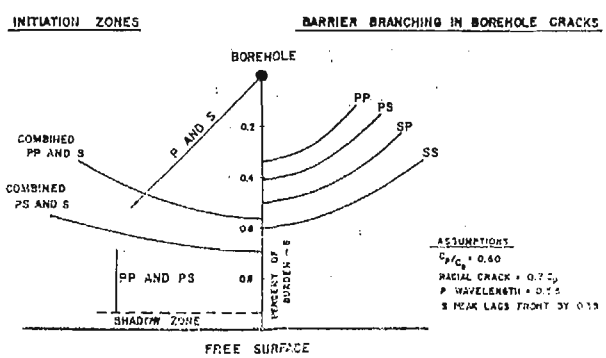

Fig. 7. Schematic showing regions in which stress waves can initiate cracks if a natural flaw is present

surface flaws exist. These were made by lightly tapping a sharp knife into the model when it was prepared. In this frame we see that cracks from the flaws close to the borehole have been initiated by the outgoing wave systems. These cracks are propagating in a radial direction. In Figure 6, 135 μsec after detonation, it can be seen that cracks at all of the small flaw locations have been initiated by outgoing and reflected stress waves. By studying the full sequence of photographs from the experiment it was possible to determine which wave system initiates the flaws and how the stress waves control the direction of the cracks. Figure 7 summarizes the regions where flaws are initiated by the outgoing, reflected, and combined wave systems.

4. A Dynamic Photoelastic Investigation of Gas and Oil Well Stimulation by Means of Explosives

From the very beginning of our oil and natural gas industry, owners and operators have attempted to recover a greater percentage of oil and gas from their wells. If the reservoir is not highly fractured, then drainage is poor and much of the oil and gas remains trapped in the rock. An early technique to fracture the formation used nitroglycerin explosive which was lowered into the producing zone and detonated. The results were mixed, but in many cases recovery was enhanced. Analysis done since the oil shortage of the early seventies has shown however that explosives can damage the well bore and actually impede the flow of gas or oil because of fine material trapped in the fractures, and the residual compressive hoop stresses. Other modern methods have also evolved for well stimulation. These include hydraulic fracturing with numerous combinations of liquids, gases, and liquefied gases. In general these processes are quasi-static; only a few fractures are formed, and their direction is controlled by the in-situ stresses. Propellants also have been used, since it is possible to control to some degree the rate of chemical reaction, thus reducing the well bore damage. See for example Cuderman and Northrop (1984). However, propellants are 10 to 20 times more expensive than explosives. Because of these deficiencies there has been renewed interest in developing a stimulation method that would provide an optimum pressure pulse in terms of peak pressure, total duration and time to peak pressure. In our laboratory we have investigated placing the explosive away from the zone

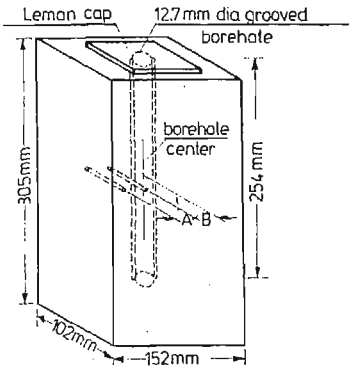

Fig 8.

to be stimulated (thus minimizing damage) and using the well bore geometry and end conditions to tailor the explosive pressure. For further background see Fourney, Barker, and Holloway (1981) and Fourney, Holloway, and Simha (1984).

The techniques developed, called stem induced fracturing, have been studied using the Cranz-Schardin camera and dynamic photoelasticity. A typical model used in the testing is depicted in Fig. 8. The models, made from 102 mm thick PMMA, were placed in front of the camera so that fractures initiated at the tips of notches along the borehole length would be seen as a plane. Stem induced fracturing utilizes a highly decoupled charge placed in the bottom of the borehole. Small piezoelectric transducers were used to monitor the pressures within the borehole and within the propagating fractures, such as at locations *A* and *B*.

Four frames from a typical 16 frame test are presented in Figure 9. PMMA, commercially known as plexiglas, is a birefringent material. The camera was fitted with circular polaroids to permit areas of high stresses to be identified during the testing. The black fringes in Figure 9 are isochromatics. For the test shown, a 250 mg charge was used. Frame 5, Figure 9a, shows the fracture location 90 μs after detonation (the fracture is the dark

Fig. 9. Sequence from stem induced fracturing test

bladder-shaped area near the bottom of the model). Notice the two long straight fringes located in the upper third of the model. These show the *P*-wave in the PMMA which is being generated by the gas shock wave traveling up the borehole from the detonation. Each fringe makes an angle of 40° with the borehole wall, from which it is calculated that the ratio of shock wave speed to *P*-wave speed in the PMMA is 1.19. Note that there are two bright areas in the borehole, one at the bottom where the charge was detonated, and one near the top, at the stem. The bright area at the stem is due to an increase in pressure and temperature, caused by the shock wave reflection from the stem. Light is emitted due to ionization of the gas at that location. The camera used to record the photographs is such that light emitted from any area within the field of view will be visible in all 16 frames, so it is not possible to determine at what time the light flash occurred.

By the time Frame 6 (Fig. 9b) was recorded, just 23 μs later at 113 μsec, a fracture is seen to have initiated at the stemming area and has grown considerably. At this time the charge area fracture continues to grow, but at a much slower rate. By 191 μsec (Fig. 9c) the fracture that originated at the stem is larger than the charge area fracture. Frame 15 (Fig. 9d) shows the stem area fracture beginning to engulf the arrested charge area fracture at 296 μsec after detonation.

Figure 10 is a sketch showing how the fracture grew from frame to frame. The times at which each frame was photographed and the velocities computed from the crack front

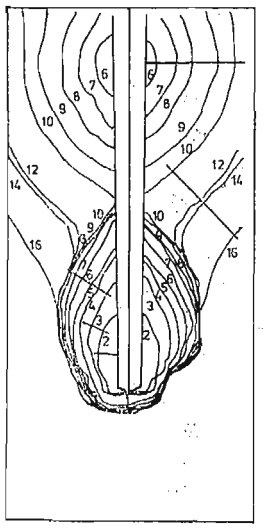

Frame No.	Time (μsec)	Velocities between frames (m/s)	
		Charge area	Stem area
1	12.5		
2	34.0	530*	
3	57.0	350	
4	80.5	299	
5	89.5	317	
6	112.5	320	266*
7	140.0	183	451
8	163.5	128	442
9	190.5		558
10	214.5		314
12	246.5		733
14	271.5		167
16	322.5		512

* Velocity probably low since fracture was not likely to initiate at the same instant the time count started

Fig. 10

positions are indicated. Numbers on the sketch represent the frame sequence and the straight lines indicate directions along which the velocity measurements were made. Notice how quickly the charge area fracture slows and arrests, while the stemming area fracture continues to propagate at a somewhat erratic but high speed. The high velocity between Frames 10 and 12 occured because the fracture reached the free edge of the model. The reason for the low velocity between Frames 12 and 14 is not clear. In many similar tests

using PMMA and geologic materials, this stem induced fracturing machanism has been shown to be very efficient in initiating and advancing fractures.

The important point of this work is that explosives can be efficiently used to generate long fractures from well bores, which in turn connect natural fractures, thus increasing the yield from a well.

Acknowledgement

The authors wish to thank the National Science Fundation and the U.S. Department of Energy for partial sponsorship of the work. Some of the work by Mr. Wilson was performed in partial fulfillment of the requirements for the degree of Doctor of Philosophy at the University of Maryland.

References

1. D. B. BARKER, and W. L. FOURNEY, *Photoelastic Investigation of Fragmentation Mechanisms. Part II-Flaw Initiated Network*, Report to U.S. National Science Foundation, Photomechanics Laboratory, Mechanical Engineering Dept., University of Maryland 1978.
2. J. F. CUDERMAN, and D. A. NORTHROP, *A Propellant-Based Technology for Multiple Fracturing Wellbores To Enhance Gas Recovery: Application and Results in Devonian Shale*, Proceedings, SPE/DOE/GRI Unconventional Gas Recovery Symposium, Pittsburgh, Pa., pp. 77 - 86, 1984.
3. W. L. FOURNEY, D. B. BARKER, and D. C. HOLLOWAY, *Model Studies of Explosive Well Stimulation Techniques*, Int. J. Rock Mech. Min. Sci. & Geomech. Abstr., Vol. 18, pp. 113 - 127, 1981.
4. W. L. FOURNEY, D. C. HOLLOWAY, and K. R. Y. SIMHA, *Model Investigation of Borehole Pressure Distribution*, Proceedings, SPE/DOE/GRI Unconventional Gas Recovery Symposium, Pittsburgh, Pa., pp. 497 - 506, 1984.
5. D. C. HOLLOWAY, and A. M. PATACCA, *Application of Holography to a Study of Wave Propagation in Rock*, Report to National Science Foundation by the Photomechanics Laboratory, Mechanical Engineering Department, University of Maryland, College Park, Md. 1975.
6. D. C. HOLLOWAY, W. L. FOURNEY, and A. M. PATACCA, *A Study of Surface Wave Propagation by Holographic Interferometry*, Experimental Mechanics, Vol. 17, No. 8, August, pp. 281 - 289, 1977.
7. D. C. HOLLOWAY, and W. H. WILSON, *Experimental Investigation of Dynamic Surface Response to Explosive Loading*, Proceedings, First International Symposium on Rock Fragmentation by Blasting, Lulea, Sweden, pp. 605 - 624, 1983.
8. W. F. RILEY, and J. W. DALLY, *Recording Dynamic Fringe Patterns with a Cranz-Schardin Camera* Experimental Mechanics, Vol. 9, No. 8, pp. 27 - 33, 1969.

Р е з ю м е

ПРИМЕНЕНИЕ ГОЛОГРАФИЧЕСКОЙ ИНТЕРФЕРОМЕТРИИ И ФОТОУПРУГОСТИ ДЛЯ ИССЛЕДОВАНИЯ ДИНАМИЧЕСКИХ ЗАДАЧ ГЕОТЕХНИКИ

В работе обсуждено применение голографической интерферометрии и фотоупругости для исследований взрывов и возникающих эффектов в геологических задачах.

Особенно методом голографической интерферометрии была исследована задача возникновения волн напряжений на поверхности детонации и их воздействия на неверхностные канавы.

Динамическая фотоупругость, при применении камеры Кранца-Шадрина была применена для исследования влияния преривности возрывного материала, а также для определения оптимального распределения взрывного материала при добывании нефты и газа.

Streszczenie

ZASTOSOWANIE INTERFEROMETRII HOLOGRAFICZNEJ I ELASTOOPTYKI DO BADANIA DYNAMICZNYCH PROBLEMÓW GEOTECHNIKI

W pracy opisano zastosowanie interferometrii holograficznej i elastooptyki do badań wybuchów i ich efektów w zastosowaniach geologicznych. Metodą interferometrii holograficznej badano szczególnie problem tworzenia się fal naprężeń na powierzchni detonacji i oddziaływania na rowy powierzchniowe.

Elastooptyka dynamiczna, przy zastosowaniu kamery Kranza-Schadrina była stosowana do badania wpływu nieciągłości materiału wybuchowego oraz do wyznaczenia optymalnego rozkładu materiału wybuchowego dla wydobycia gazu i ropy.

Praca została złożona w Redakcji dnia 20 kwietnia 1985 roku